

Bcl-x_L Retrotranslocates Bax from the Mitochondria into the Cytosol

Frank Edlich,¹ Soojay Banerjee,¹ Motoshi Suzuki,² Megan M. Cleland,¹ Damien Arnoult,⁴ Chunxin Wang,¹ Albert Neutzner,³ Nico Tjandra,² and Richard J. Youle^{1,*}

¹Surgical Neurology Branch, NINDS

²Laboratory of Molecular Biophysics, NHLBI

National Institutes of Health, Bethesda, MD 20892, USA

³Universitätsspital Basel, Augenklinik, Basel 4031, Switzerland

⁴INSERM U1014, Hôpital Paul Brousse, Villejuif cedex 94807, France

*Correspondence: youle@helix.nih.gov

DOI 10.1016/j.cell.2011.02.034

SUMMARY

The Bcl-2 family member Bax translocates from the cytosol to mitochondria, where it oligomerizes and permeabilizes the mitochondrial outer membrane to promote apoptosis. Bax activity is counteracted by prosurvival Bcl-2 proteins, but how they inhibit Bax remains controversial because they neither colocalize nor form stable complexes with Bax. We constrained Bax in its native cytosolic conformation within cells using intramolecular disulfide tethers. Bax tethers disrupt interaction with Bcl-x_L in detergents and cell-free MOMP activity but unexpectedly induce Bax accumulation on mitochondria. Fluorescence loss in photobleaching (FLIP) reveals constant retrotranslocation of WT Bax, but not tethered Bax, from the mitochondria into the cytoplasm of healthy cells. Bax retrotranslocation depends on prosurvival Bcl-2 family proteins, and inhibition of retrotranslocation correlates with Bax accumulation on the mitochondria. We propose that Bcl-x_L inhibits and maintains Bax in the cytosol by constant retrotranslocation of mitochondrial Bax.

INTRODUCTION

Bcl-2 proteins control many pathways of programmed cell death in multicellular animals. Members of the Bcl-2 family can be grouped in prosurvival Bcl-2-like proteins and proapoptotic Bax-like members (Chipuk and Green, 2008; Cory and Adams, 2002; Youle and Strasser, 2008). The functions of Bcl-2 family members can be regulated by a diverse group of “BH3-only” proteins that initiate the proapoptotic activities of Bax-like proteins (Chipuk and Green, 2008).

Bax resides in the cytoplasm of healthy cells and translocates to the mitochondrial outer membrane (MOM) upon apoptosis induction (Wolter et al., 1997), where it causes cytochrome c (cyt c) release from the mitochondrial intermembrane space and mitochondrial dysfunctions (Gross et al., 1998; Martinou et al., 1999; Wang et al., 2001; Wei et al., 2001). The three

concomitant events that characterize the commitment of a cell to apoptosis, Bax oligomerization, cyt c release, and breakdown of the interconnected mitochondrial network, are tightly linked to the process of Bax translocation.

An early “rheostat model” proposed that Bax is restrained by heterodimerization with prosurvival Bcl-2 family proteins (Korsmeyer et al., 1993). However, this view could not be reconciled with experimental evidence of monomeric Bax residing in the cytoplasm of healthy cells, in contrast to the mitochondrial localization of Bcl-2 on the MOM (Hsu et al., 1997; Hsu and Youle, 1998). Although interactions between Bax and prosurvival Bcl-2 proteins control Bax activity (Fletcher et al., 2008), the question remains: How do prosurvival Bcl-2 proteins regulate Bax from a distance without interacting with Bax in the cytoplasm?

In an attempt to resolve the dilemma of Bax regulation by prosurvival Bcl-2 proteins independent of “sequestration,” BH3-only proteins have been suggested to mediate the link between cytosolic Bax and the mitochondrial prosurvival proteins. Some findings indicate that Bax can bind to and be activated by the BH3-only proteins Bim, Puma, or the proapoptotic Bcl-2 family protein tBid (Desagher et al., 1999; Kim et al., 2006; Kuwana et al., 2005; Letai et al., 2002). Accordingly, these Bax “activator” proteins are proposed to be sequestered and neutralized by prosurvival Bcl-2 family members in healthy cells. In response to apoptosis, induction “activator” proteins could be released from prosurvival Bcl-2 family proteins, perhaps by competition with other BH3-only proteins binding to prosurvival Bcl-2 family members, to activate Bax (Kim et al., 2006). Cell-free assays show a synergistic effect of tBid or Bim on Bax-mediated membrane permeabilization, suggesting a role of both proteins in direct Bax activation (Kuwana et al., 2005; Wei et al., 2000). Apoptosis assays with Bid/Bim DKO MEFs and the phenotypes of the corresponding knockout mice show that many apoptosis pathways do not depend on activity of either tBid or Bim (Willis et al., 2007), whereas the analysis of Bid/Bim/Puma TKO cells shows an effect on apoptosis induction by several stimuli (Ren et al., 2010). However, direct binding between Bax and BH3-only proteins in cells is not readily apparent (Walensky et al., 2006).

Further evidence indicates that Bax interacts with prosurvival Bcl-2 proteins and suggests that BH3-only proteins play a role in

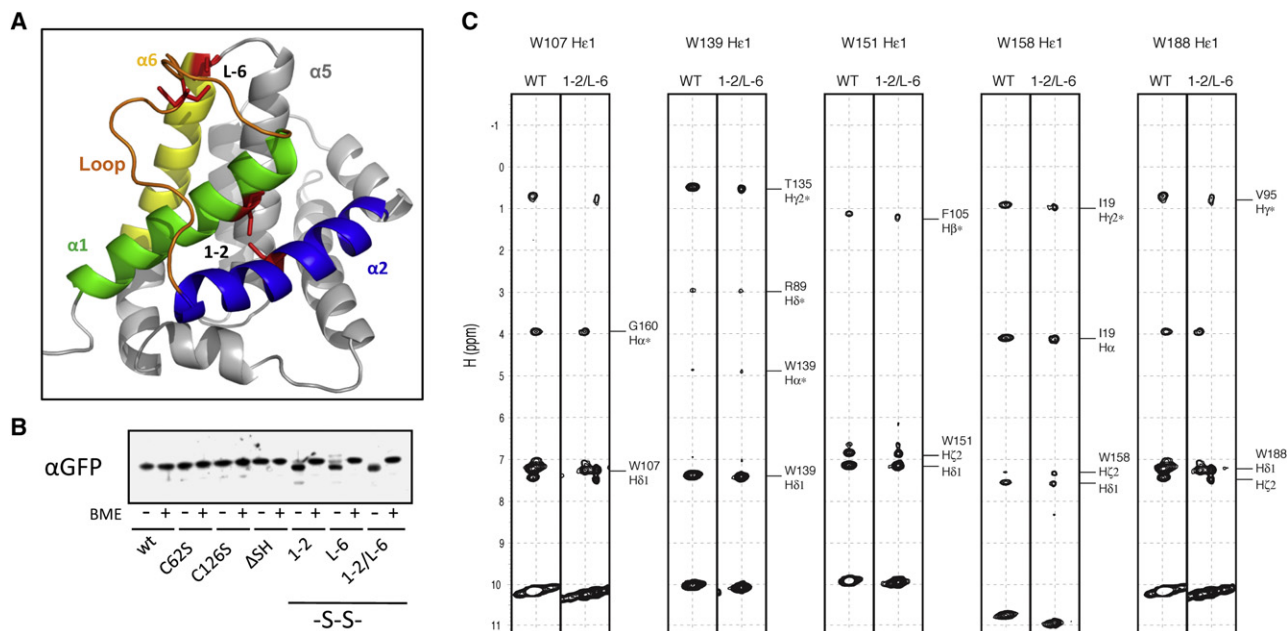


Figure 1. Disulfide Bonds Constrain Bax in Its Inactive Fold

(A) Depiction of the three-dimensional structure of Bax (PDB, 1F16) containing cysteine substitutions for F30, E44, L63, and P130 (red sticks) to form disulfide bonds constraining α helices 1 (green) and 2 (1-2) and the loop (orange) between α helices 1 and 2 and α helix 6 (L-6) using Pymol software (DeLano Scientific LLC). Helix 2 is depicted in blue; helix 6, in yellow. See also Figure S1A.

(B) The disulfide bond formation of cysteine GFP-Bax variants in HCT116 Bax/Bak DKO cells was analyzed by SDS-PAGE and western blot of cell extracts in the presence and absence of β -mercaptoethanol (BME) using rabbit α -GFP antibody. See also Figures S1B–S1D.

(C) Selected spectra of NOESY experiment for Bax 1-2/L-6 and WT Bax. Each strip for the indicated tryptophan side chain labeled above was extracted from the ^{15}N -edited 3D NOESY spectra. Left panels were obtained from WT Bax, whereas the right panels were from Bax 1-2/L-6. Cross-peaks for NOE interactions for WT Bax were identified from ^{15}N -edited 3D NOESY as well as $^{13}\text{C}/^{15}\text{N}$ -edited 4D NOESY. Identical strips are displayed for Bax 1-2/L-6, confirming that the fold of the Bax variant is the same as that of WT Bax. See also Figures S1E and S1F.

interfering with the heterodimer formation between Bax and pro-survival Bcl-2 proteins, rather than directly activating Bax (Chen et al., 2005; Willis et al., 2005, 2007). Bax also has been found to undergo major conformational changes to integrate in lipid bilayers where membrane-bound Bax can form stable complexes with either tBid or Bcl-x_L (Dlugosz et al., 2006; Lovell et al., 2008). However, the models of anti- and proapoptotic Bcl-2 family member interaction fail to explain why during apoptosis inhibition increased Bcl-x_L concentrations do not result in an accumulation of Bax on mitochondria in complex with Bcl-x_L.

We report here a mechanism of antiapoptotic Bcl-2 family member inhibition of Bax activation and apoptosis whereby Bax in the cytoplasm of nonapoptotic cells continually binds to mitochondria and retrotranslocates back to the cytoplasm through interaction with Bcl-x_L.

RESULTS

Disulfide Bonds Constrain the Inactive Bax Conformation

The activation of Bax involves major changes in its protein conformation that are linked to mitochondrial localization and integration into the MOM. We sought to hinder conformational changes involving α helices 1 and 2 of Bax containing the BH3 motif to analyze their involvement in Bax activity. To constrain

Bax in its inactive conformation, we substituted to cysteine residues F30 and L63, which are in close proximity, to form an intramolecular disulfide bond between α helices 1 and 2 (1-2) (Figure 1A and Figure S1A available online). We also changed E44 and P130 to cysteines to constrain the flexible loop between α helices 1 and 2 to the tip of helix 6 (L-6). In addition, the intrinsic cysteine residues C62 and C126 were substituted by serine residues (Bax Δ SH) to avoid interference with the engineered disulfide bonds.

Previous reports have shown that disulfide bonds can form in the reducing environment of the cytosol (Bessette et al., 1999; Locker and Griffiths, 1999; Østergaard et al., 2004; Schouten et al., 2002). We examined whether the disulfide bonds 1-2 and L-6 are formed in Bax expressed in HCT116 Bax/Bak DKO cells by SDS-PAGE and western blot in the absence and presence of β -mercapto-ethanol (BME). Wild-type Bax and the Bax variants C62S, C126S, and C62/126S (Δ SH) migrate similarly with and without BME, whereas Bax variants with one or two engineered disulfide bonds (1-2, L-6, and 1-2/L-6) migrate faster in the absence of BME than WT Bax (Figure 1B). The decreased Stokes radius of the denatured Bax variants in the absence of BME indicates that the engineered disulfide bonds form in Bax within cells.

We confirmed the absence of free SH groups in Bax 1-2/L-6 by thiol trapping using a maleimide derivative with a 10 kDa mPEG

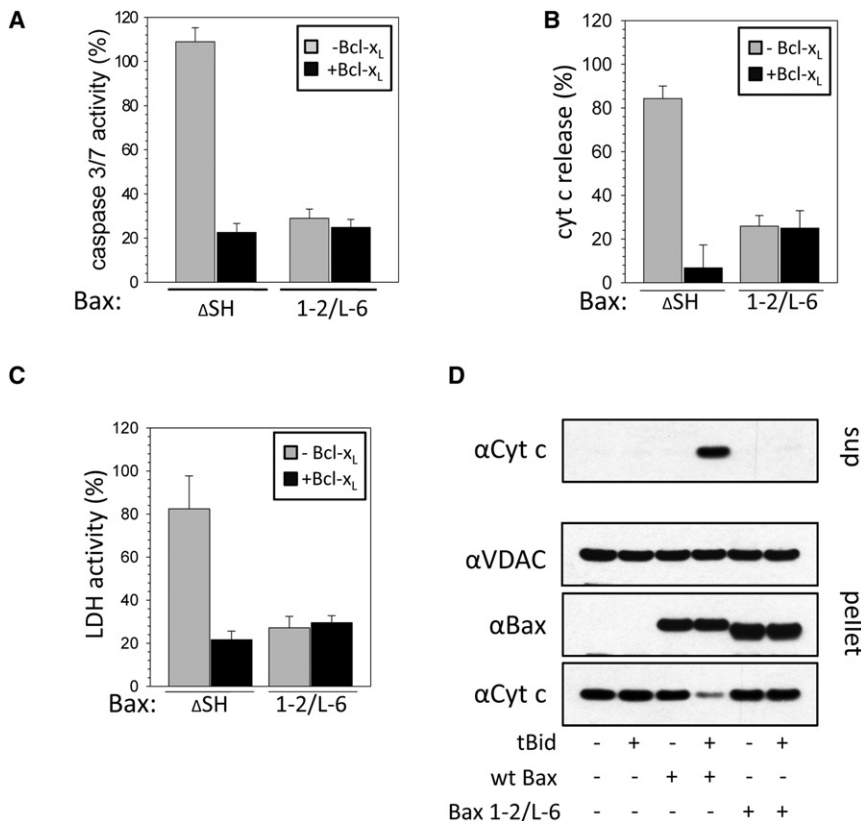


Figure 2. Constraining Bax Prevents Proapoptotic Activity and Inhibition by Bcl-x_L

(A) Staurosporine (STS, 1 μM)-induced apoptosis activity of Bax ΔSH and Bax 1-2/L-6 based on caspase 3/7 activity measured in HCT116 Bax/Bak DKO cells relative to the activity obtained with WT Bax and normalized to mock-transfected cells. Results were obtained without (gray) or with (black) overexpressed Bcl-x_L. Data represent averages ± SD; n ≥ 5 × 5 wells.

(B) Cyt c release from the mitochondria analyzed microscopically in HCT116 Bax/Bak DKO cells expressing different GFP-Bax variants after apoptosis induction by 1 μM STS. Results were obtained without (gray) or with (black) overexpressed Bcl-x_L. Data represent averages ± SD from triplicates. n ≥ 125 cells.

(C) LDH activity measured after transfecting HCT116 Bax/Bak DKO cells with different GFP-Bax variants for 24 hr and inducing apoptosis with 1 μM STS for 16 hr relative to the activity obtained with cells transfected with GFP-Bax WT and normalized to mock-transfected cells. Results were obtained with (black) or without (gray) overexpressed Bcl-x_L. Data represent averages ± SD. n ≥ 4 × 5 wells.

(D) Cyt c release by WT Bax and Bax 1-2/L-6 (see also Figures S2A and S2B) in absence and presence of tBid from purified mitochondria. Cyt c is monitored in the supernatant and pellet by western blot. VDAC serves as a loading control. See also Figures S2C and S2D.

fusion (mPEG-MAL) while WT Bax becomes modified (Figure S1B). The analysis of Bax variants expressed in HCT116 Bax/Bak DKO cells with mPEG-MAL also showed free SH groups in GFP-Bax WT that are absent in GFP-Bax ΔSH (Figure S1C). Thiol trapping of either GFP-Bax 1-2 or GFP-Bax L-6 shows pools of unmodified but also of modified protein, whereas GFP-Bax 1-2/L-6 remains unaltered, suggesting stabilization of a compact Bax fold by the two disulfide bonds, thereby shielding the disulfides from the reducing environment of the cytosol. The redox potential of the disulfide bonds of this Bax variant was determined to be lower than -370 mV (Figure S1D), consistent with their formation in the cytosol (Schafer and Buettner, 2001).

We analyzed the conformation of recombinant Bax 1-2/L-6 by NMR in comparison to WT Bax. NMR chemical shift (δ) is sensitive to molecular conformation. Differences of chemical shifts (Δδ) between WT Bax and Bax 1-2/L-6 can be used as a probe of conformational differences of these two molecules. Noticeable differences in chemical shifts of the backbone amide proton and nitrogen are present but are limited to the regions where mutations were introduced (Figure S1E). The absence of significant differences that are not associated with mutations indicates that the global structure of Bax 1-2/L-6 is essentially the same as that of WT Bax. In addition, nuclear Overhauser effect (NOE) is direct evidence of molecular structure, as it reports two protons within 5 Å. The NOE spectra from five tryptophan side chains were unaffected by the substitutions (Figure 1C). Noteworthy, the side chain Hε1 of Trp158 located at the loop between α6

and α7 helices showed NOEs to Hα and Hγ2 of Ile19 that is 11 residues away from the F30C mutation site, where both Ile19 and Cys30 are located within the α1 helix. In WT Bax, the same NOEs between Trp158 Hε1 and Ile19 Hγ2 and Hα were observed. We also found that the regions of flexibility of Bax 1-2/L-6 are the same as WT Bax, only differing with reduced dynamics at the L-6 disulfide tether (Figure S1F). Thus, the intramolecular tethers stabilize the native and inactive conformation in Bax 1-2/L-6 that is similar to inactive WT Bax (see also Supplemental Results).

Disulfide Bonds Inhibit Bax Activity and Regulation by Bcl-x_L

We tested the influence of stabilizing the inactive conformation of Bax in cells by measuring caspase 3/7 activity. Staurosporine (STS)-induced caspase activity in HCT116 Bax/Bak DKO cells expressing Bax ΔSH is similar to WT Bax-expressing cells (data not shown) and is prevented by Bcl-x_L overexpression (Figure 2A). In parallel to the caspase activity assay in Bax ΔSH-expressing cells, STS induces increased cyt c release and cell death indicated by the release of LDH that is inhibited by Bcl-x_L overexpression. Similar activities were obtained in HCT116 Bax KO cells with Bax ΔSH or additional single cysteine substitution of either F30, E44, L63, or P130, showing that the substitutions used in Bax 1-2/L-6 do not interfere with Bax activity without disulfide bond formation (data not shown). In all three assays, Bax 1-2/L-6 lacks STS-inducible activity (Figures

2A–2C). However, in the presence of Bcl-x_L (Figure 2B) or in the absence of apoptosis induction (Figures S2A and S2B), overexpression of Bax 1-2/L-6 induced cyt c release more than overexpression of WT Bax. The ability of recombinant Bax 1-2/L-6 to induce cyt c release was also tested using mitochondria isolated from Bax/Bak DKO MEFs (Figure 2D). In this assay, recombinant WT Bax causes the release of cyt c from isolated mitochondria in the presence of tBid. Recombinant Bax 1-2/L-6 fails to induce cyt c release even in the presence of tBid. Thus, the intramolecular tethers in Bax 1-2/L-6 decrease its activation by BH3-only proteins and regulation by Bcl-x_L. Although Bax and Bcl-x_L do not interact in the cytoplasm of cells, their interaction can be induced *in vitro* by detergents (Hsu and Youle, 1997). We assessed whether constraining Bax with intramolecular tethers interferes with this interaction. Though WT Bax and Bcl-x_L interact in the presence of different detergents at concentrations greater than CMC, Bax 1-2/L-6 forms heterodimers with Bcl-x_L only in Triton X-100, Triton X114, and dodecyl maltoside (Figure S2C and Supplemental Results). Thus, intramolecular tethers can interfere with detergent-induced Bcl-x_L binding.

Tethered Bax Localizes to the Mitochondria

Inactive Bax resides mainly in the cytoplasm. Upon activation, Bax forms foci at the tips and constriction sites of mitochondria that is temporally associated with mitochondrial outer membrane permeabilization (MOMP) and cyt c release (Karbowski et al., 2004). Like WT Bax, Bax Δ SH is found predominantly in the cytosol of transfected HCT116 Bax/Bak DKO cells and translocates to mitochondria upon apoptosis stimulation (Figures 3A–3C). Surprisingly, Bax 1-2/L-6 is not located in the cytosol and smoothly coats the mitochondria in 99% of healthy cells and remains unchanged in the presence of apoptotic stimuli (Figures 3A–3C). Whereas Bcl-x_L overexpression prevents the localization of Bax Δ SH to the mitochondria after apoptosis induction, GFP-Bax 1-2/L-6 circumscribes the mitochondria even on Bcl-x_L overexpression (Figure S3A and Supplemental Results). Cell fractionation confirms that, in contrast to Bax Δ SH, most Bax 1-2/L-6 is found in the heavy membrane (HM) fraction in the absence of apoptosis induction (Figure 3D). Tethered Bax is largely carbonate extractable, suggesting that it binds mitochondria but does not integrate into the MOM.

Wild-Type, but Not Tethered, Bax Retrotranslocates from the Mitochondria into the Cytoplasm

Why does tethered Bax localize to mitochondria in healthy cells despite adopting an inactive conformation? Although WT Bax resides mainly in the cytoplasm of healthy cells, a fraction localizes to mitochondria but, in contrast to mitochondrially embedded Bax found following apoptosis induction, is carbonate extractable (Desagher et al., 1999). We hypothesized that the mitochondrial Bax pool could be in equilibrium with cytosolic Bax in healthy cells, which could be disrupted by Bax tethers. In an attempt to distinguish between cytosolic and mitochondrial Bax and compare WT Bax with Bax 1-2/L-6, we performed fluorescence loss in photobleaching (FLIP) with different GFP-Bax variants expressed in HCT116 Bax/Bak DKO cells. To this end, we repeatedly bleached a region in the nucleus of a transfected cell (Figure 4A, white square). The declining GFP

fluorescence in the targeted cell was followed by assigning regions of interest in the cytoplasm (green circle) and on the mitochondria (red and blue circles) in Figure 4A. GFP-Bax readily crosses the nuclear envelope, and cytosolic GFP fluorescence of the targeted cell was bleached rapidly by FLIP, whereas the neighboring reference cell fluorescence (black circle) remained stable, ruling out photobleaching during imaging (Figures 4A and 4B). After reducing the cytosolic GFP-Bax signal, the mitochondrial GFP-Bax pool was readily apparent (Figure 4B, arrows). The decay of mitochondrial GFP-Bax fluorescence by FLIP occurs within 660 s following a first-order kinetic at a rate ($4.7 \pm 0.1 \times 10^{-3} \text{ s}^{-1}$) that is notably slower than the loss in cytosolic fluorescence (Figures 4B and 4C and Figure S4A). Interestingly, Bcl-x_L overexpression causes more than an 80% increase in the rate of mitochondrial fluorescence reduction during FLIP at comparable levels of Bax expression (Figures 4B–4E). The loss in mitochondrial GFP-Bax fluorescence during FLIP suggests that Bax could exist in an equilibrium between mitochondrial and cytosolic states (Figure 4D).

The presence of MG132 had no effect on GFP-Bax fluorescence loss with or without Bcl-x_L (Figure S4B), indicating that proteasomal degradation does not account for the decrease in mitochondrial fluorescence during FLIP. To directly assess Bax return to the cytosol from mitochondria, we analyzed fluorescence recovery after photobleaching (FRAP) of cytosolic GFP-Bax (Figure S4C). Following the bleach, GFP-Bax fluorescence increases in the cytosol by about 25% after 400 s following a first-order kinetic (Figure 4F). Overexpression of Bcl-x_L increases the cytosolic reappearance of GFP-Bax fluorescence more than 2-fold when mitochondrial postbleach GFP-Bax levels were comparable (Figure S4D). We examined whether continual retrotranslocation is balanced by continual binding of Bax to mitochondria in healthy cells. By photobleaching half of a cell expressing GFP-Bax (Figure 4H), we quantified the binding of Bax to mitochondria over the subsequent 10 min (Figures 4G and 4H and Figure S4E). Bax WT translocates to mitochondria at a rate of $4.7 \pm 0.2 \times 10^{-3} \text{ s}^{-1}$, consistent with an equilibrium between on and off rate.

Although FLIP analyses appear to measure an increase in mitochondrial Bax off rates by Bcl-x_L, it could be suggested that WT Bax and Bcl-x_L may compete for the same binding site on the mitochondria, causing increased Bax retrotranslocation into the cytoplasm. This possibility was tested by analyzing the effect of untagged Bax overexpression on GFP-Bax retrotranslocation (Figure S4F). In contrast to Bcl-x_L overexpression, Bax slightly decreases the GFP-Bax retrotranslocation rate ($4.4 \pm 0.1 \times 10^{-3} \text{ s}^{-1}$), indicating no competition between Bax and Bcl-x_L for MOM binding. In the presence of untagged Bax, the overexpression of Bcl-x_L accelerates GFP-Bax retrotranslocation ($7.0 \pm 0.2 \times 10^{-3} \text{ s}^{-1}$) but significantly less than without untagged Bax ($8.6 \pm 0.4 \times 10^{-3} \text{ s}^{-1}$), suggesting that Bax can compete with GFP-Bax for Bcl-x_L-mediated retrotranslocation. Mitochondrial Bax retrotranslocation into the cytoplasm dependent on the Bcl-x_L concentration may provide a rationale for the mitochondrial accumulation of Bax 1-2/L-6. The intramolecular tethers in Bax 1-2/L-6 may interfere with Bcl-x_L-mediated retrotranslocation, as they also disrupt the interaction between Bax and Bcl-x_L in some detergents. We applied FLIP to analyze

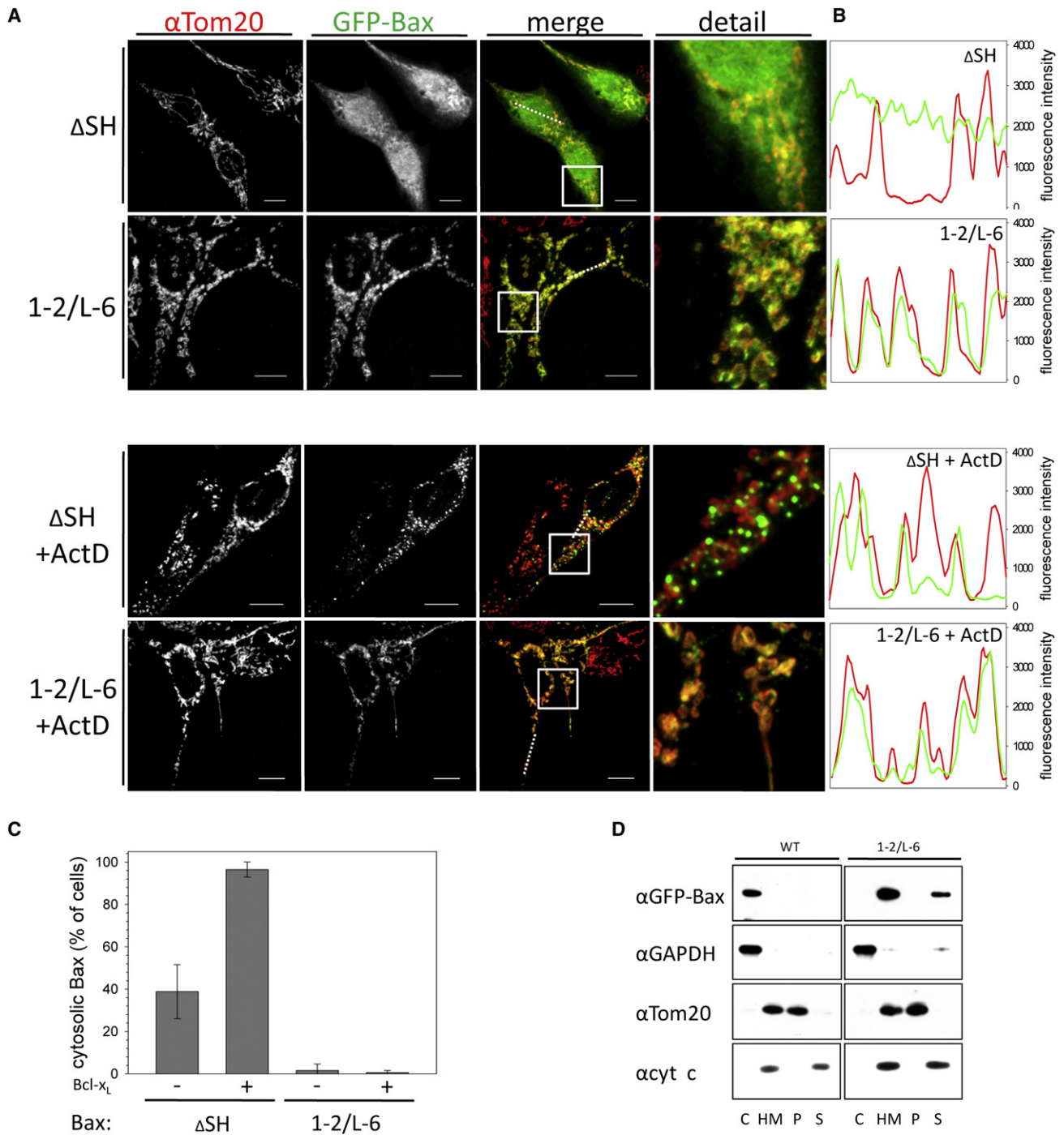


Figure 3. Bax 1-2/L-6 Localizes to the Mitochondria

(A) Confocal imaging of HCT116 Bax/Bak DKO transfected with GFP-Bax Δ SH or GFP-Bax 1-2/L-6 with or without treatment with 1 μ M actinomycin D (ActD) for 2 hr. Q-VD was used to prevent caspase activation. GFP-fluorescence is depicted in the second panels and in green in the merge and detail, whereas α -Tom20 staining is shown in the left panels and in red in the merged and detail images. In the merged and detail images, colocalization is shown in yellow. The white line in the lower-right corner of every image is the scale of 10 μ m. White broken lines in the merge images show the section analyzed in the line scans (B). The merged section depicted in the detail panel is indicated by a white box.

(B) Line scans show the fluorescence intensities of GFP-Bax signals (green) and mitochondria stained by α -Tom20 staining (red) along the selected line (A) in cells transfected with GFP-Bax Δ SH or Bax 1-2/L-6 either with or without ActD treatment.

(C) Quantification of confocal images of HCT116 Bax/Bak DKO cells transfected with either GFP-Bax Δ SH or 1-2/L-6 showing predominantly cytosolic Bax cell populations in percent of the total cell population after 2 hr treatment with 1 μ M ActD with or without Bcl- x_L coexpression. Data represent averages of triplicates \pm SD; $n \geq 150$ cells. See also Figure S3.

Bax 1-2/L-6 retrotranslocation, bleaching the low GFP-Bax 1-2/L-6 fluorescence in the cytoplasm, as was done for WT GFP-Bax. Mitochondrial GFP-Bax 1-2/L-6 fluorescence intensity was not significantly reduced by repeated bleaching (Figures 5A and 5B). In contrast to WT Bax, Bcl-x_L overexpression did not detectably increase the retrotranslocation of Bax 1-2/L-6 in a 660 s time frame (Figures 5A and 5B). Thus, Bax 1-2/L-6 is deficient in retrotranslocation. We examined the role of helix 9 in Bax 1-2/L-6 binding to mitochondria. Bax 1-2/L-6 displayed the same sensitivity to S184 mutations as WT Bax (Nechushtan et al., 1999) (Figures S5A and S5B), indicating that helix 9 is required for Bax 1-2/L-6 binding to mitochondria.

Bax Retrotranslocation Depends on BH3 Interactions with Prosurvival Bcl-2 Proteins

We tested the effect of different Bcl-2 family members on Bax retrotranslocation. Overexpression of Bcl-2 and Mcl-1 accelerated Bax retrotranslocation similarly to Bcl-x_L (Figure 6A and Figure S6A). In contrast, the BH3-only protein Bim reduced the rate of Bax retrotranslocation more than 3-fold to $1.3 \pm 0.2 \times 10^{-3} \text{s}^{-1}$ in HCT116 Bax/Bak DKO cells that did not contain Bax foci. Endogenous Bak expression tested by comparing HCT116 Bax/Bak DKO and Bax KO cells has no influence on Bax retrotranslocation (Figure 6A and Figure S6A). After MOMP or in the presence of the viral Bax inhibitor vMIA (Arnoult et al., 2004), WT Bax retrotranslocation is inhibited (see also Supplemental Results and Figures S6B–S6E).

To analyze whether binding of prosurvival Bcl-2 proteins to Bax is required to mediate Bax retrotranslocation, we examined Bcl-x_L G138A, a variant that is deficient in Bax binding and apoptosis inhibition (Desagher et al., 1999; Dlugosz et al., 2006; Sedlak et al., 1995). In contrast to WT Bcl-x_L, G138A failed to accelerate retrotranslocation of GFP-Bax when expressed at levels comparable to WT Bcl-x_L (Figures 6B and 6C). Furthermore, the Bcl-2/Bcl-x_L inhibitor ABT-737 (Oltersdorf et al., 2005) reduced the rate of Bax retrotranslocation by more than 75%, suggesting that endogenous Bcl-2 family members mediate Bax retrotranslocation (Figure 6D and Figure S7A). These results indicate the involvement of direct interactions between prosurvival Bcl-2 proteins and Bax for retrotranslocation.

The Bax variant D68R has been previously shown to exhibit insensitivity toward Bcl-2/Bcl-x_L inhibition and potent proapoptotic activity (Fletcher et al., 2008). Interestingly, Bax D68R constitutively localizes to the mitochondria of HCT116 Bax/Bak DKO cells in the absence of apoptosis stimuli (Figures 6E and 6F). Bax D68R localizes to the mitochondria even in cells not displaying cyt c release (Figure 6F). We analyzed whether Bax D68R retrotranslocation could be accelerated by overexpression of the prosurvival Bcl-2 proteins Bcl-2, Bcl-x_L, and Mcl-1. Bax D68R retrotranslocates at less than half the rate of WT Bax (Figure 6G), whereas the S184V substitution in helix 9, which also increases the mitochondrial Bax pool, only slightly

decreases Bax retrotranslocation (see also Supplemental Results and Figures S7B and S7C). In contrast to WT Bax, the retrotranslocation rate of D68R is only slightly increased by Bcl-2 and Bcl-x_L overexpression from $2.1 \pm 0.1 \times 10^{-3} \text{s}^{-1}$ to about $3.9 \times 10^{-3} \text{s}^{-1}$, whereas overexpression of Mcl-1 does not accelerate Bax D68R retrotranslocation (Figure 6G). The ability of the different prosurvival Bcl-2 proteins to increase Bax D68R retrotranslocation correlates with the relative affinities of Mcl-1, Bcl-2, and Bcl-x_L for Bax D68R (Fletcher et al., 2008). The diminished retrotranslocation of Bax D68R extends the results obtained with tethered Bax 1-2/L-6, indicating the importance of prosurvival Bcl-2 protein interactions with the BH3 domain of Bax, which is further indicated by the retrotranslocation of a Bcl-x_L chimera with its helices 2 and 3 replaced by the corresponding Bax helices (George et al., 2007). The retrotranslocation rate of this chimera is similar to the rate of Bax (Figure S7D).

The possibility of Bcl-x_L retrotranslocation was analyzed by performing FLIP with HCT116 Bax/Bak DKO cells expressing GFP-Bcl-x_L. GFP-Bcl-x_L localizes in these cells predominantly to the mitochondria (Figure S7E) and retrotranslocates in the absence of Bax with a low rate ($1.4 \pm 0.1 \times 10^{-3} \text{s}^{-1}$) from the mitochondria into the cytoplasm (Figure 6H). Overexpression of Bax accelerates Bcl-x_L retrotranslocation about 3.5-fold, suggesting that they interact on mitochondria, retrotranslocate together, and dissociate in the cytosol. Interestingly, ABT-737 increases the Bcl-x_L retrotranslocation rate (Figure S7F).

Bax 1-2/L-6 Adopts a 6A7-Positive Fold on the Mitochondria

Upon translocation to the mitochondria during apoptosis, WT Bax exposes an epitope consisting of P13–I19 at the N terminus of helix 1 for the monoclonal antibody 6A7 that is not accessible in cytosolic and mitochondrial WT Bax in healthy cells (Hsu and Youle, 1998). This change in the 6A7 epitope correlates with foci formation and cyt c release (Nechushtan et al., 1999). Despite constitutive mitochondrial localization, Bax 1-2/L-6 fails to form foci.

Surprisingly, Bax 1-2/L-6 is 6A7 positive in some, but not all, cells (Figures 7A and 7B) while circumscribing the mitochondria (Figure 3A). Only a subset of Bax 1-2/L-6 on the mitochondria adopts a 6A7-positive fold as inferred by the Pearson's coefficient of about 0.7 (Figure 7C). The pool of 6A7-positive cells transfected with Bax 1-2/L-6 is slightly decreased by Bcl-x_L overexpression, whereas almost 100% of WT Bax-expressing cells are 6A7 negative with Bcl-x_L overexpression (Figure 7B). Interestingly, Bax 1-2/L-6 changes to its 6A7-positive conformation gradually over 24 hr on the mitochondria of healthy cells (Figure 7D).

Although the disulfide tethers in Bax 1-2/L-6 would reduce the conformational flexibility of its N-terminal part, they do not completely block Bax from undergoing a conformational change on the mitochondria that results in the exposure of the 6A7

(D) GFP-Bax WT and GFP-Bax 1-2/L-6 localization in HCT116 Bax/Bak DKO cells analyzed by SDS-PAGE and western blot after fractionation into cytosol (C) and heavy membrane fraction (HM) and subjecting membrane-bound proteins to carbonate extraction and analyzing pellet (P) and supernatant (S) with rabbit α -GFP, rabbit α -GAPDH, mouse α -cyt c, and rabbit α -Tom20 antibodies.

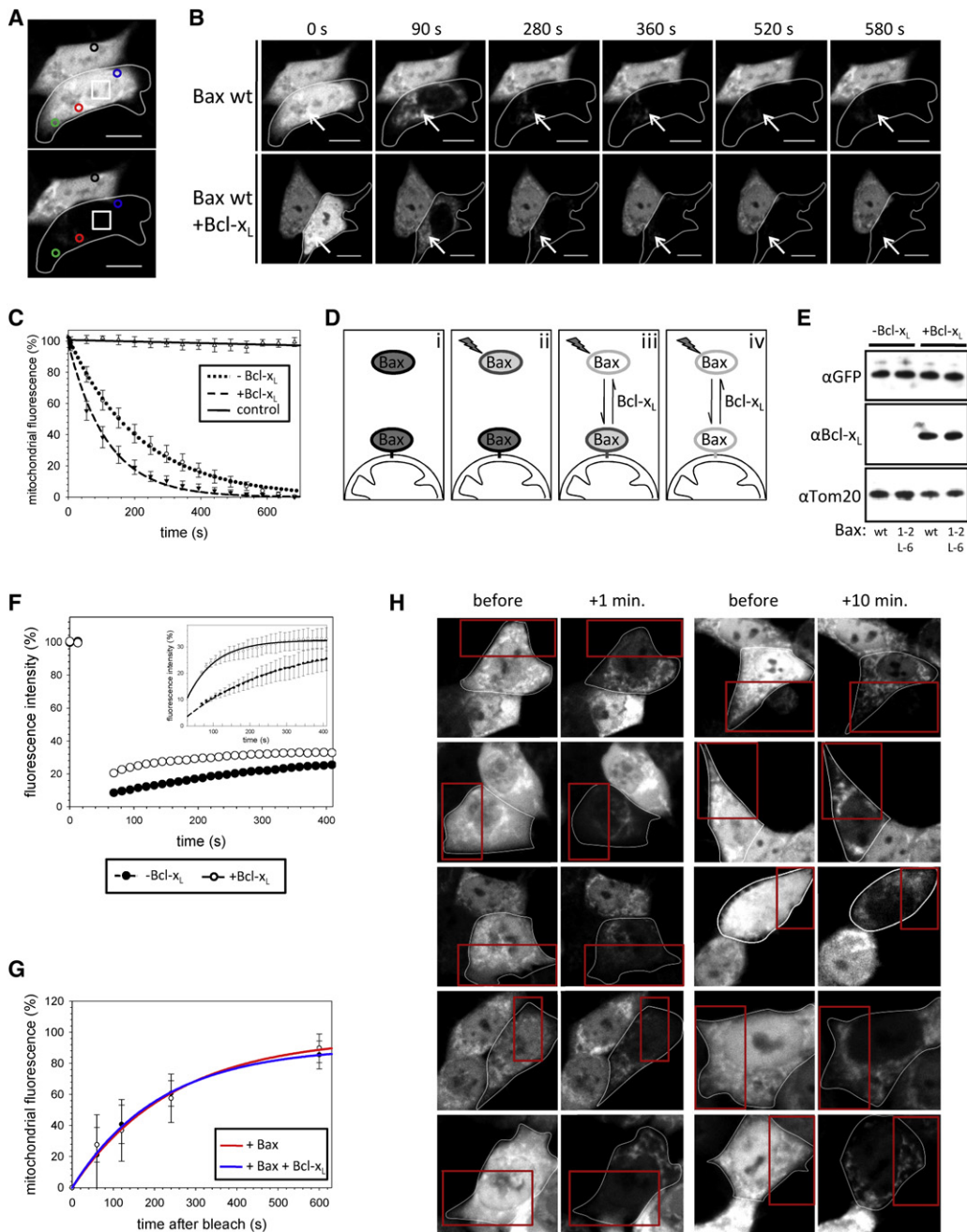


Figure 4. Wild-Type Bax Retrotranslocates from the Mitochondria into the Cytoplasm

(A) GFP-Bax fluorescence is monitored in a FLIP experiment with 15 bleachings at 488 nm in the region marked as square. Changes in Bax fluorescence on the mitochondria are detected in two areas (red circle and blue circle, respectively), and an additional area monitors changes in the cytosolic fluorescence (green circle), whereas a ROI measurement in the neighboring cell serves as a control for cell-specific bleaching (black circle).

(B) FLIP of GFP-Bax in the absence (top) and presence (bottom) of overexpressed Bcl-x_L diminishes GFP-Bax fluorescence in the cytoplasm of both targeted cells (circled) completely after 90 s, and GFP fluorescence is detected only on the mitochondria (arrows). The mitochondrial GFP-Bax signal in the presence of overexpressed Bcl-x_L is lower at 90 s. Time points in seconds are displayed above the pictures.

(C) Bcl-x_L increases the rate of Bax retrotranslocation. FLIP of mitochondrial GFP-Bax in the absence (circle) and presence (filled triangle) of overexpressed Bcl-x_L. Fluorescence of the neighboring cell is shown as control (open triangle). Data represent averages ± SEM from 20 ROI measurements per condition. See also Figure S4A.

(D) Prior to FLIP, GFP-Bax localizes to mitochondria and cytosol (i). FLIP bleaches cytosolic Bax (ii), but in addition, the mitochondrial fluorescence is diminished because bleached Bax molecules translocate to the mitochondria while fluorescent GFP-Bax retrotranslocates into the cytoplasm dependent on Bcl-x_L (iii). After an extended time of 15 FLIP iterations, all GFP-Bax molecules are bleached (iv).

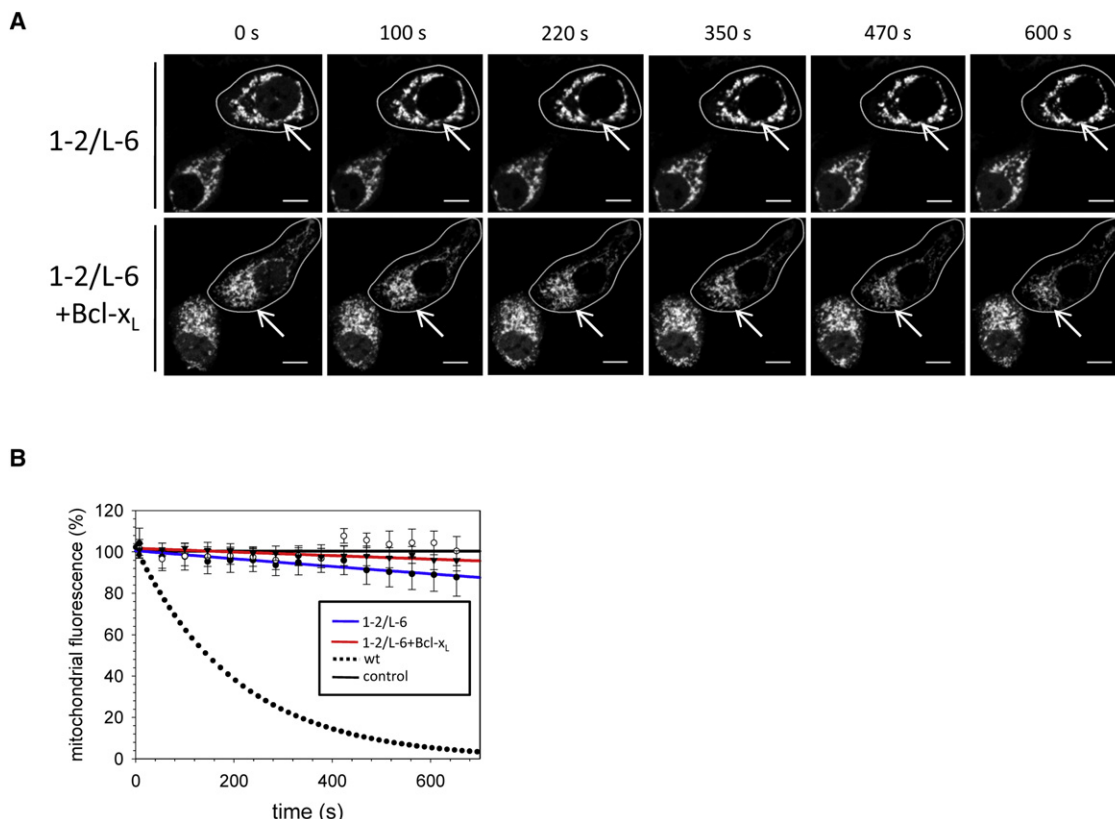


Figure 5. Bax 1-2/L-6 Is Deficient in Retrotranslocation

(A) Time course recorded for GFP-Bax 1-2/L-6 in the absence (top) and presence (bottom) of overexpressed Bcl-x_L in FLIP experiments. FLIP diminishes GFP-Bax 1-2/L-6 in the cytoplasm of a targeted cell (circled) quickly in parallel to WT Bax, but mitochondrial signals (arrows) remain stable. Time points in seconds during FLIP iterations are displayed above the pictures. See also Figure S5.

(B) FLIP of mitochondrial GFP-Bax 1-2/L-6 as shown in (A) in the absence (blue, filled circles) and presence (red, filled triangles) of overexpressed Bcl-x_L. The neighboring cell fluorescence (open circles) and cells transfected with GFP-Bax WT (filled circles) serve as controls. Data represent averages ± SEM from 20 (Bax 1-2/L-6 – Bcl-x_L) and 18 (Bax 1-2/L-6 + Bcl-x_L) ROI measurements.

epitope. Because Bax 1-2/L-6 does not show induced apoptotic activity, the 6A7-positive conformational change smoothly coating mitochondria seems to be an intermediate step en route to activation, likely correlating with spontaneous induction of cytochrome c release (Figures S2A and S2B) upstream of foci formation. As WT Bax does not reach the 6A7-positive state when circumscribing mitochondria in healthy cells, the prolonged association of Bax 1-2/L-6 with mitochondria may be the stimulus. Subsequent conformational rearrangements inhibited by the tethers likely are associated with foci formation.

DISCUSSION

Prosurvival Bcl-2 proteins prevent apoptosis by inhibiting Bax and Bak. They block Bax translocation from the cytosol to the mitochondria, Bax oligomerization, and MOMP. Paradoxically, prosurvival Bcl-2 proteins on the mitochondria stabilize Bax localization in the cytosol, without forming stable heterodimeric complexes. Bax regulation by Bcl-2 thus creates a spatial paradox that has been addressed by previous models of Bax activation (Kim et al., 2006; Willis et al., 2007).

(E) Similar levels of GFP-Bax WT and GFP-Bax 1-2/L-6 expression in HCT116 Bax/Bak DKO cells in the presence and absence of Bcl-x_L overexpression analyzed by SDS-PAGE and western blot using rabbit α-GFP, mouse α-Bcl-x_L, and rabbit α-Tom20 antibodies.

(F) GFP-Bax fluorescence is recovering in the cytoplasm after a single bleach at 488 nm (inset shows magnification), and Bcl-x_L is increasing the rate of this fluorescence intensity regain, consistent with the FLIP experiments. Data represent averages ± SEM from 22 (–Bcl-x_L) and 16 (+Bcl-x_L) ROI measurements. See also Figures S4C and S4D.

(G) Translocation of Bax to the mitochondria of healthy cells analyzed by cell bleaching (Figure S4E). Recovery of mitochondrial GFP-Bax WT fluorescence 1, 2, 4, and 10 min after bleach was compared in the absence (red, open circles) or presence (blue, filled circles) of Bcl-x_L to unbleached mitochondria in 12 different cells per data point ± SD.

(H) HCT116 Bax/Bak DKO cells expressing GFP-Bax WT imaged before the analysis by bleaching (first and third panels from the left; see also Figure S4E). Then the cells (circled) were bleached in the area in the red squares. After 1 or 10 min, the fluorescence in the cytoplasm was bleached and the cells were imaged (second and fourth panels, respectively) for analysis (in G).

See also Figures S4B and S4F.

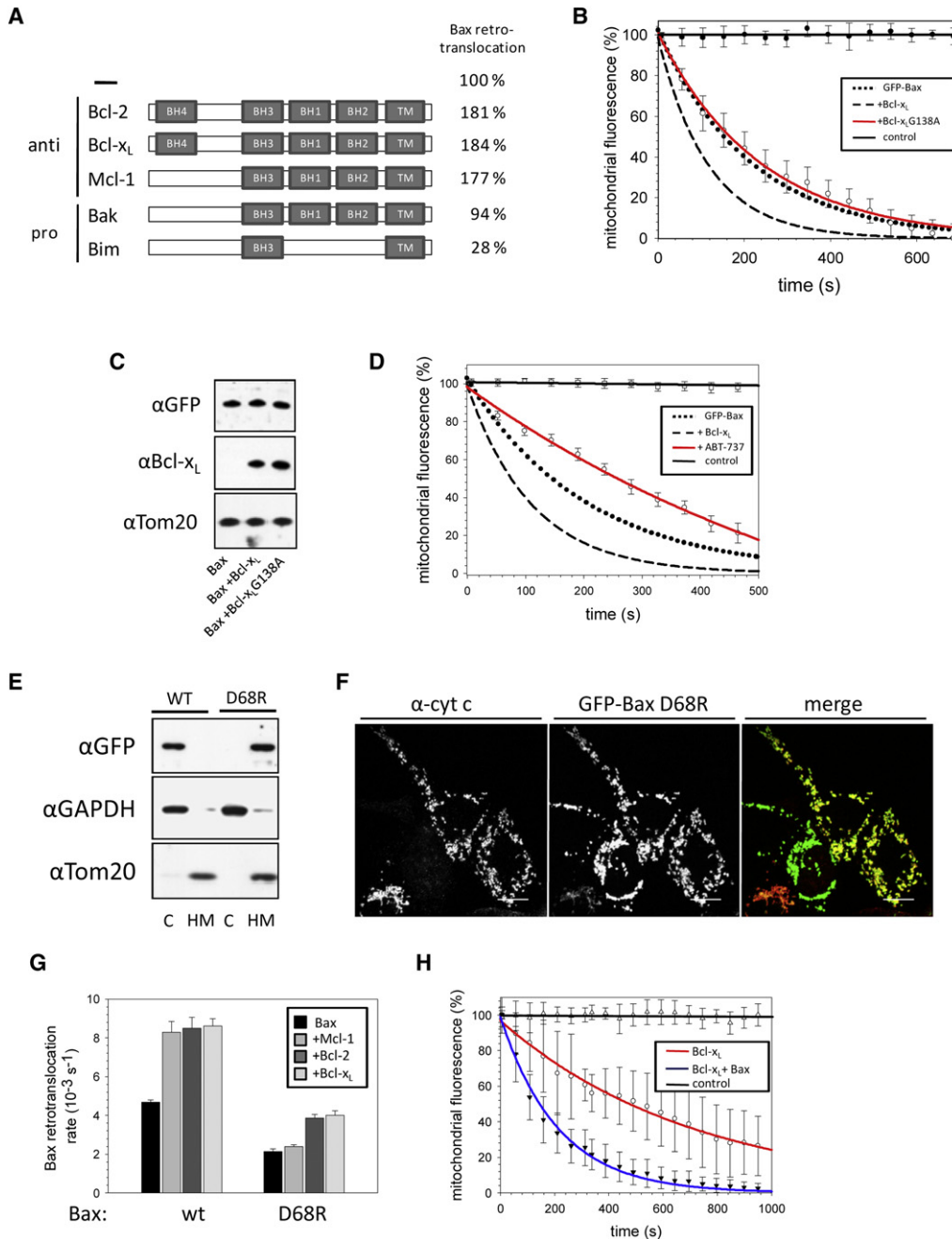


Figure 6. Bax Retrotranslocation Depends on Interactions between BH3 and Prosurvival Bcl-2 Proteins

(A) Influence of Bax interaction partners on retrotranslocation. Prosurvival and proapoptotic Bax interaction partners are displayed as a schematic depiction of their Bcl-2 homology domain (BH) organization, with the C-terminal transmembrane domains (TM) on the right. Bax retrotranslocation rates in the presence and absence of overexpressed Bcl-2, Bcl-x_L, Mcl-1, or Bim measured in HCT116 Bax/Bak DKO or in HCT116 Bax KO for measurements in the presence of endogenous Bak are depicted on the right in %. See also Figure S6A.

(B) Interactions between Bcl-x_L and Bax are implicated in retrotranslocation. FLIP of GFP-Bax in the absence (filled circles) or presence of Bcl-x_L WT (dashed line) or Bcl-x_L G138A (red, open circles). The neighboring cell fluorescence serves as control (line). Data display averages ± SEM from 12 ROI measurements per condition.

(C) Similar expression levels of Bcl-x_L variants in HCT116 Bax/Bak DKO cells analyzed by SDS-PAGE and western blot using mouse α-Bcl-x_L and rabbit α-GFP to probe for GFP-Bax overexpression and rabbit α-Tom20 antibodies.

(D) FLIP experiment with GFP-Bax in absence (filled circles) and presence (dashed line) of overexpressed Bcl-x_L or Bcl-x_L inhibitor ABT-737 (red, open circles). The fluorescence of the neighboring cell serves as control (line). Data represent averages ± SEM from 24 (+ABT-737) and 10 (+DMSO) ROI measurements. See also Figure S7A.

We propose a model of continuous Bax retrotranslocation from mitochondria that is consistent with results from numerous labs. We find that Bax translocates constantly to the mitochondria in healthy cells, where prosurvival Bcl-2 proteins, such as Bcl-x_L, bind Bax and retrotranslocate it back into the cytoplasm, thereby stabilizing the inactive Bax conformation (Figures 7E and 7F). Bcl-x_L and Bax both retrotranslocate from mitochondria and accelerate the rate of each other's retrotranslocation after transient interaction on mitochondria, perhaps through *trans*-sequestration of the C-terminal tails (Jeong et al., 2004). Evidence for direct interaction is based on the inhibition of Bax retrotranslocation when the Bax-Bcl-x_L binding is disrupted by: (1) the G138A mutation in the hydrophobic groove of Bcl-x_L (Sedlak et al., 1995), (2) the D68R mutation in the BH3 domain of Bax (Fletcher et al., 2008), and (3) the Bcl-x_L inhibitor ABT-737 (Oltersdorf et al., 2005). The interaction between Bax and Bcl-x_L requires prior conformational changes in the N-terminal part of Bax because preventing these conformational changes by intramolecular tethers disrupts interaction with Bcl-x_L in detergents and Bax retrotranslocation.

The absence of retrotranslocation results in Bax 1-2/L-6 accumulation on the mitochondria in healthy cells. Wild-type Bax, however, only accumulates on mitochondria when the activities of prosurvival Bcl-2 proteins are blocked by BH3-only proteins, such as Bim, or by ABT-737. Bax accumulated on mitochondria upstream of MOMP can dissipate by retrotranslocation if prosurvival Bcl-2 proteins become available again, as observed when cells reattach to substrate following transient anoikis (Gilmore et al., 2000).

Conformational changes of Bax on the mitochondria during apoptosis involve the N terminus of Bax and can be detected using the monoclonal antibody 6A7. Despite its reduced apoptotic activity, tethered Bax eventually adopts a 6A7-positive fold but does not form mitochondrial foci. Although in cell-free assays tethered Bax completely lacks tBID activated MOMP, consistent with the lack of apoptosis-induced activation in cells, tethered Bax can spontaneously induce some degree of MOMP within cells even in the presence of Bcl-x_L, likely through this 6A7-positive form. Because the 6A7 antibody can compete for Bcl-x_L binding to Bax (Hsu and Youle, 1998), a 6A7-positive conformation of WT Bax may normally exist, circumscribing mitochondria that remains undetectable because 6A7 binding is sterically blocked by Bcl-x_L bound to Bax. Bax conformational changes in α helices 1 and 2 could be a normal consequence of Bax binding to the mitochondria perhaps stimulated by lipid interactions (Kuwana et al., 2002). If not retrotranslocated, mitochondrial WT Bax becomes active due to further conformational changes and oligomerization to cause MOMP (Figure 7F).

In addition to a reduced Bax retrotranslocation (off rate), mitochondrial Bax accumulation could also result from an increase in the Bax translocation (on rate), which may depend on direct Bax activation by BH3-only proteins (Kuwana et al., 2005). Even the steady-state binding of Bax to mitochondria in healthy cells may result from the activity of residual levels of BH3-only proteins in healthy cells. Bax binding to the MOM appears to be influenced by the exposure of the C-terminal membrane anchor (Gavathiotis et al., 2010), which may also depend on isomerization of the prolyl bond preceding P168 and its acceleration by the PPLase Pin1 (Shen et al., 2009). Bax translocation to the MOM, however, seems not to be influenced by Bcl-x_L.

Despite the robust interaction of Bax and Bcl-x_L in detergents (Hsu and Youle, 1998) and in membranes (Dlugosz et al., 2006), increased concentrations of prosurvival mitochondrial-bound Bcl-2 proteins in cells do not result in Bax accumulation on mitochondria. In contrast, Bax can be directly bound and inhibited by the viral protein vMIA that accumulates Bax on the mitochondria as it inhibits apoptosis (Arnoult et al., 2004). In healthy cells, the subcellular location of Bax depends on constant retrotranslocation of mitochondrial Bax into the cytosol by prosurvival Bcl-2 proteins. Minimization of a mitochondrial Bax pool that is susceptible for activation is likely to prevent apoptosis and explains the spatial paradox of Bcl-2 protein inhibition of Bax.

EXPERIMENTAL PROCEDURES

Cell Culture and Transfection

HCT116 cells were cultured in McCoy's 5A medium supplemented with 10% heat-inactivated fetal bovine serum and 10 mM HEPES in 5% CO₂ at 37°C. HCT116 Bax/Bak DKO cells were obtained by deletion of the Bak gene by homologous recombination in the HCT116 Bax^{-/-} cells (C.W. and R.J.Y., unpublished data). Cells were transfected with PolyJet (SigmaGen) or Lipofectamine LTX (Invitrogen) typically with 100 ng of the GFP-Bax construct according to the manufacturer's instructions, and cells were incubated for 6–8 hr for confocal imaging. For western blot, cells were harvested 8 hr after transfection.

Confocal Microscopy

HCT116 Bax/Bak DKO cells were seeded on a chambered coverglass (Thermo Scientific) in McCoy's 5A medium (10 mM HEPES), grown for 20 hr, transfected, and incubated for 6–8 hr. The cells were then fixed with 4% paraformaldehyde solution for 10 min and washed with PBS. The fixed cells were permeabilized with Triton X-100 for 15 min at room temperature. For double-immunofluorescence staining, cells were first incubated with 5% BSA in PBS for 1 hr at room temperature, followed by incubation with appropriate primary antibodies (anti-Tom20 and anti-6A7 antibodies) in 5% BSA solution for 2 hr, and probed with an Alexa-594- and Alexa-647-conjugated secondary antibody (Invitrogen). Confocal analysis was performed on a Zeiss 510 META confocal LSM microscope equipped with argon (458/488/514 nm lines) and HeNe (543/633 nm) lasers. For live cell experiments measuring the recovery

(E) GFP-Bax WT and GFP-Bax D68R localization in HCT116 Bax/Bak DKO cells analyzed by SDS-PAGE and western blot after fractionation into cytosol (C) and heavy membrane fraction (HM) with rabbit α -GFP, rabbit α -GAPDH, and rabbit α -Tom20 antibodies.

(F) Confocal images of HCT116 Bax/Bak DKO cells transfected with GFP-Bax D68R (center, green in the merge) and stained for cyt c (left, red in the merge). Colocalization between Bax D68R and cyt c is shown as yellow in the merge (right) when cyt c is not released from the mitochondria without apoptotic stimuli. The white line in the lower-right corner of every image is the scale of 10 μ m.

(G) Retrotranslocation rates measured for Bax WT and Bax D68R in the absence (black) and presence of Mcl-1 (gray), Bcl-2 (dark gray), or Bcl-x_L (light gray). Data represent averages \pm SD. See also Figures S7B and S7C.

(H) FLIP analysis of GFP-Bcl-x_L in the absence (red, open circles) and presence (blue, filled triangles) of overexpressed Bax (see also Figures S7E and S7F). The fluorescence of the neighboring cell serves as control (line). Data represent averages \pm SEM from 15 (–Bax) and 15 (+Bax) ROI measurements. See also Figures S6B–S6E and Figure S7D.

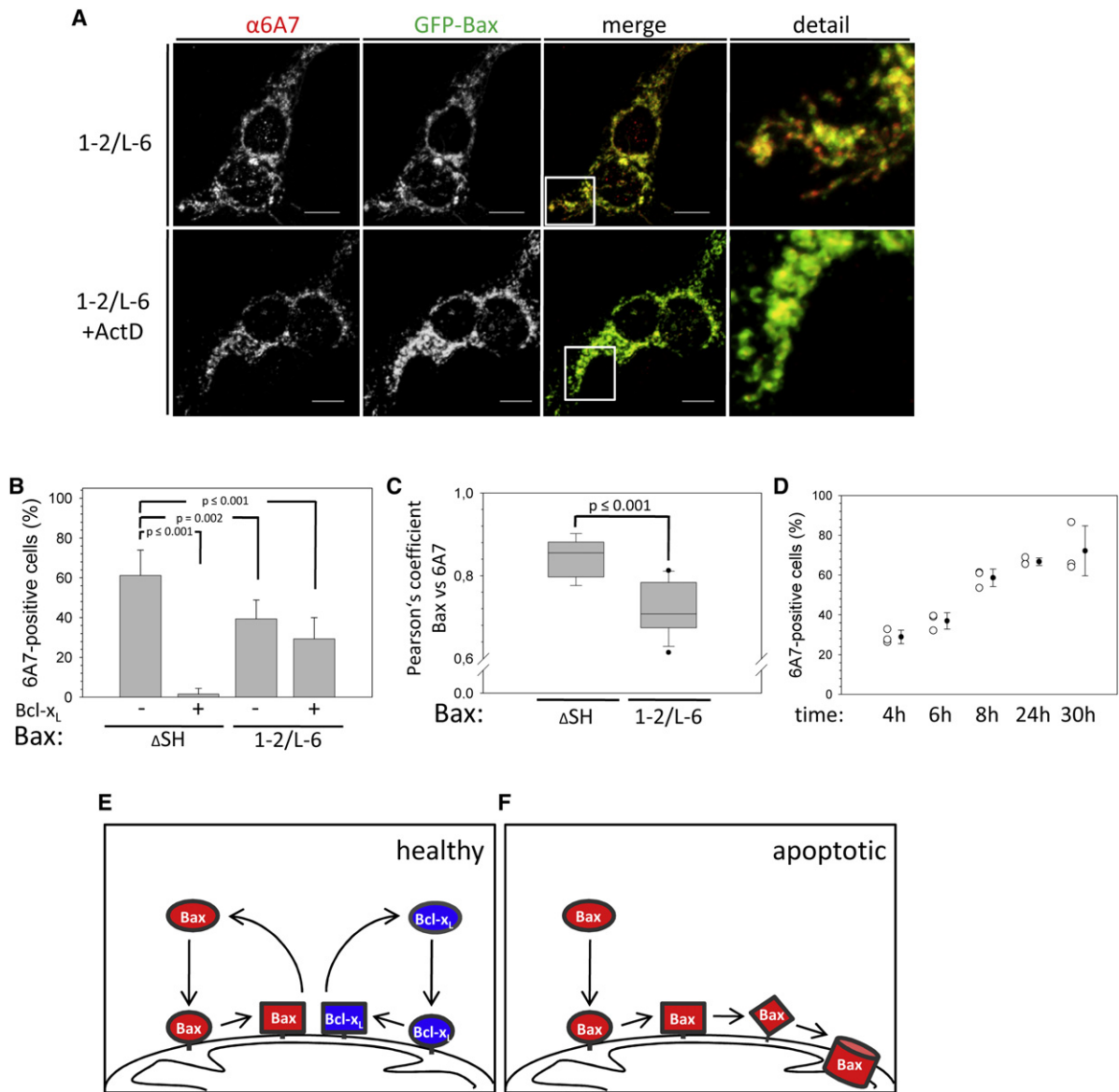


Figure 7. Mitochondrial Bax 1-2/L-6 Is 6A7 Positive

(A) Confocal imaging of HCT116 Bax/Bak DKO cells transfected with GFP-Bax 1-2/L-6 in the presence and absence of ActD (1 μ m) treatment for 2 hr. Q-VD was used to prevent caspase activation. α -6A7 staining is shown in the left panels or in red in the merged and detailed pictures on the right. GFP-Bax 1-2/L-6 is depicted in the second panels or in green in the merge and detail panels, where colocalization is shown in yellow. The white lines show the scale of 10 μ m. The merged section depicted in the detail panel is indicated by a white box.

(B) α -6A7 staining is quantified in HCT116 Bax/Bak DKO cells expressing GFP-Bax Δ SH or GFP-Bax 1-2/L-6 with or without Bcl-x_L overexpression. Data represent averages from triplicates \pm SD; $n \geq 150$ cells. p values according to the unpaired Student's t test for the comparison with Bax WT in the absence of overexpressed Bcl-x_L are depicted.

(C) Comparison of the Pearson's coefficient for the colocalization between α -6A7 staining and GFP fluorescence in HCT116 Bax/Bak DKO cells transfected with either GFP-Bax Δ SH or 1-2/L-6. The confidence range is depicted as box \pm SD with the mean (line) of the data set. Dots represent the most extreme data points for GFP-Bax 1-2/L-6. $n \geq 10$ cells. The p value for both data sets according to the unpaired Student's t test is depicted.

(D) Time-dependent changes in α -6A7 staining monitored by confocal imaging in HCT116 Bax/Bak DKO cells expressing GFP-Bax 1-2/L-6 in % of total expressing cell population. Individual measurements are displayed as open circles with the mean shown as a black circle \pm SD.

(E) Bax (red) and Bcl-x_L (blue) constantly translocate to the mitochondria and coretrotranslocate back into the cytosol, stabilizing cytosolic Bax in healthy cells. Retrotranslocation requires a conformational change in Bax.

(F) In the absence of free Bcl-x_L, mitochondrial Bax may undergo further conformational changes that can lead to Bax activity or integration into the membrane.

after FRAP, one ROI within the nucleus of a cell of interest was photobleached with the argon laser at 100% intensity. Recovery of fluorescence in the cytoplasm was monitored immediately after photobleaching by imaging the bleached cell in 20 s intervals with low laser intensity (1%). The results were normalized setting the starting fluorescence to 100% signal.

For Bax translocation assay, the cells were incubated with mitotracker-far red for 10 min prior to analysis. Approximately half of an analyzed cell was bleached with high laser power (100%) for 17.5 ms. After either 1, 2, 4, or 10 min, the cytoplasm of the cell was bleached a second time for 25 ms with high laser power. After the bleaching, two different ROI each were assigned for unbleached and bleached mitochondria.

FLIP

In FLIP experiments, a single spot with a diameter of 1 μm within the nucleus was repeatedly bleached with two iterations of 100% power of a 488 nm laser line (100% output) using a Zeiss LSM510 META with 63 \times PlanFluor lens. The average diameter of a single z axis plane varied between 2 and 2.5 μm . Two images were collected after each bleach pulse, with 30 s between bleach pulses. After collecting 30 images, two separate measurements on the mitochondria were taken to analyze the fluorescence loss. Unbleached control cells were monitored for photobleaching due to image acquisition. The rate of loss in fluorescence on the mitochondria was calculated from fluorescence intensity measurements using the Zeiss LSM software. The fluorescence intensities were normalized by setting the initial fluorescence to 100% signal. Plots are shown as normalized fluorescence over time.

Apoptosis Activity Assays

For caspase 3/7 measurements, HCT116 Bax/Bak DKO cells were transfected with different Bax constructs in 96-well plates and incubated with or without 1 μM STS for 4 hr. Then, Apo-ONE caspase 3/7 Reagent (Promega) was added according to manufacturer's protocol. The samples were incubated for 16 hr in the dark and then analyzed by measuring the fluorescence with an excitation wavelength of 488 nm and an emission wavelength range of 530 nm. For LDH measurements, 96-well plates with HCT116 Bax/Bak DKO cells transfected with different Bax constructs were incubated with 1 μM STS for 24 hr. Then, 50 μl of the supernatant from each well was transferred in a new plate, and 50 μl of the substrate mix (Promega, cytotox 96 kit) was added to each well of the plate. After 30–60 min, 50 μl of stop solution was added, and the absorbance at 490 nm was detected.

SUPPLEMENTAL INFORMATION

Supplemental Information includes Extended Results, Extended Experimental Procedures, seven figures, and four movies and can be found with this article online at [doi:10.1016/j.cell.2011.02.034](https://doi.org/10.1016/j.cell.2011.02.034).

ACKNOWLEDGMENTS

We thank Dr. D.W. Andrews and Dr. J.-C. Martinou for helpful discussions and comments. We also thank Dr. D.R. Green for the Omi-mCherry construct. This work is supported by the Leopoldina, National Academy of Sciences, Germany (F.E.); La Ligue contre le Cancer (D.A.); the NHLBI (M.S. and N.T.); and the NINDS intramural programs.

Received: September 8, 2010

Revised: December 28, 2010

Accepted: February 15, 2011

Published: March 31, 2011

REFERENCES

Arnout, D., Bartle, L.M., Skaletskaya, A., Poncet, D., Zamzami, N., Park, P.U., Sharpe, J., Youle, R.J., and Goldmacher, V.S. (2004). Cytomegalovirus cell death suppressor vMIA blocks Bax- but not Bak-mediated apoptosis by binding and sequestering Bax at mitochondria. *Proc. Natl. Acad. Sci. USA* **101**, 7988–7993.

Bessette, P.H., Åslund, F., Beckwith, J., and Georgiou, G. (1999). Efficient folding of proteins with multiple disulfide bonds in the *Escherichia coli* cytoplasm. *Proc. Natl. Acad. Sci. USA* **96**, 13703–13708.

Chen, L., Willis, S.N., Wei, A., Smith, B.J., Fletcher, J.I., Hinds, M.G., Colman, P.M., Day, C.L., Adams, J.M., and Huang, D.C. (2005). Differential targeting of prosurvival Bcl-2 proteins by their BH3-only ligands allows complementary apoptotic function. *Mol. Cell* **17**, 393–403.

Chipuk, J.E., and Green, D.R. (2008). How do BCL-2 proteins induce mitochondrial outer membrane permeabilization? *Trends Cell Biol.* **18**, 157–164.

Cory, S., and Adams, J.M. (2002). The Bcl2 family: regulators of the cellular life-or-death switch. *Nat. Rev. Cancer* **2**, 647–656.

Desagher, S., Osen-Sand, A., Nichols, A., Eskes, R., Montessuit, S., Lauper, S., Maundrell, K., Antonsson, B., and Martinou, J.-C. (1999). Bid-induced conformational change of Bax is responsible for mitochondrial cytochrome c release during apoptosis. *J. Cell Biol.* **144**, 891–901.

Dlugosz, P.J., Billen, L.P., Annis, M.G., Zhu, W., Zhang, Z., Lin, J., Leber, B., and Andrews, D.W. (2006). Bcl-2 changes conformation to inhibit Bax oligomerization. *EMBO J.* **25**, 2287–2296.

Fletcher, J.I., Meusburger, S., Hawkins, C.J., Riglar, D.T., Lee, E.F., Fairlie, W.D., Huang, D.C.S., and Adams, J.M. (2008). Apoptosis is triggered when prosurvival Bcl-2 proteins cannot restrain Bax. *Proc. Natl. Acad. Sci. USA* **105**, 18081–18087.

Gavathiotis, E., Reyna, D.E., Davis, M.L., Bird, G.H., and Walensky, L.D. (2010). BH3-triggered structural reorganization drives the activation of proapoptotic BAX. *Mol. Cell* **40**, 481–492.

George, N.M., Evans, J.J.D., and Luo, X. (2007). A three-helix homo-oligomerization domain containing BH3 and BH1 is responsible for the apoptotic activity of Bax. *Genes Dev.* **21**, 1937–1948.

Gilmore, A.P., Metcalfe, A.D., Romer, L.H., and Streuli, C.H. (2000). Integrin-mediated survival signals regulate the apoptotic function of Bax through its conformation and subcellular localization. *J. Cell Biol.* **149**, 431–446.

Gross, A., Jockel, J., Wei, M.C., and Korsmeyer, S.J. (1998). Enforced dimerization of BAX results in its translocation, mitochondrial dysfunction and apoptosis. *EMBO J.* **17**, 3878–3885.

Hsu, Y.-T., and Youle, R.J. (1997). Nonionic detergents induce dimerization among members of the Bcl-2 family. *J. Biol. Chem.* **272**, 13829–13834.

Hsu, Y.T., and Youle, R.J. (1998). Bax in murine thymus is a soluble monomeric protein that displays differential detergent-induced conformations. *J. Biol. Chem.* **273**, 10777–10783.

Hsu, Y.-T., Wolter, K.G., and Youle, R.J. (1997). Cytosol-to-membrane redistribution of Bax and Bcl-X(L) during apoptosis. *Proc. Natl. Acad. Sci. USA* **94**, 3668–3672.

Jeong, S.Y., Gaume, B., Lee, Y.J., Hsu, Y.T., Ryu, S.W., Yoon, S.H., and Youle, R.J. (2004). Bcl-x(L) sequesters its C-terminal membrane anchor in soluble, cytosolic homodimers. *EMBO J.* **23**, 2146–2155.

Karbowski, M., Arnout, D., Chen, H., Chan, D.C., Smith, C.L., and Youle, R.J. (2004). Quantitation of mitochondrial dynamics by photolabeling of individual organelles shows that mitochondrial fusion is blocked during the Bax activation phase of apoptosis. *J. Cell Biol.* **164**, 493–499.

Kim, H., Rafiuddin-Shah, M., Tu, H.C., Jeffers, J.R., Zambetti, G.P., Hsieh, J.J., and Cheng, E.H. (2006). Hierarchical regulation of mitochondrion-dependent apoptosis by BCL-2 subfamilies. *Nat. Cell Biol.* **8**, 1348–1358.

Korsmeyer, S.J., Shutter, J.R., Veis, D.J., Merry, D.E., and Oltvai, Z.N. (1993). Bcl-2/Bax: a rheostat that regulates an anti-oxidant pathway and cell death. *Semin. Cancer Biol.* **4**, 327–332.

Kuwana, T., Mackey, M.R., Perkins, G., Ellisman, M.H., Latterich, M., Schneider, R., Green, D.R., and Newmeyer, D.D. (2002). Bid, Bax, and lipids cooperate to form supramolecular openings in the outer mitochondrial membrane. *Cell* **111**, 331–342.

Kuwana, T., Bouchier-Hayes, L., Chipuk, J.E., Bonzon, C., Sullivan, B.A., Green, D.R., and Newmeyer, D.D. (2005). BH3 domains of BH3-only proteins differentially regulate Bax-mediated mitochondrial membrane permeabilization both directly and indirectly. *Mol. Cell* **17**, 525–535.

- Letai, A., Bassik, M.C., Walensky, L.D., Sorcinelli, M.D., Weiler, S., and Korsmeyer, S.J. (2002). Distinct BH3 domains either sensitize or activate mitochondrial apoptosis, serving as prototype cancer therapeutics. *Cancer Cell* 2, 183–192.
- Locker, J.K., and Griffiths, G. (1999). An unconventional role for cytoplasmic disulfide bonds in vaccinia virus proteins. *J. Cell Biol.* 144, 267–279.
- Lovell, J.F., Billen, L.P., Bindner, S., Shamas-Din, A., Fradin, C., Leber, B., and Andrews, D.W. (2008). Membrane binding by tBid initiates an ordered series of events culminating in membrane permeabilization by Bax. *Cell* 135, 1074–1084.
- Martinou, I., Desagher, S., Eskes, R., Antonsson, B., André, E., Fakan, S., and Martinou, J.C. (1999). The release of cytochrome c from mitochondria during apoptosis of NGF-deprived sympathetic neurons is a reversible event. *J. Cell Biol.* 144, 883–889.
- Nechushtan, A., Smith, C.L., Hsu, Y.-T., and Youle, R.J. (1999). Conformation of the Bax C-terminus regulates subcellular location and cell death. *EMBO J.* 18, 2330–2341.
- Oltersdorf, T., Elmore, S.W., Shoemaker, A.R., Armstrong, R.C., Augeri, D.J., Belli, B.A., Bruncko, M., Deckwerth, T.L., Dingemans, J., Hajduk, P.J., et al. (2005). An inhibitor of Bcl-2 family proteins induces regression of solid tumours. *Nature* 435, 677–681.
- Østergaard, H., Tachibana, C., and Winther, J.R. (2004). Monitoring disulfide bond formation in the eukaryotic cytosol. *J. Cell Biol.* 166, 337–345.
- Ren, D., Tu, H.-C., Kim, H., Wang, G.X., Bean, G.R., Takeuchi, O., Jeffers, J.R., Zambetti, G.P., Hsieh, J.J.D., and Cheng, E.H.Y. (2010). BID, BIM, and PUMA are essential for activation of the BAX- and BAK-dependent cell death program. *Science* 330, 1390–1393.
- Schafer, F.Q., and Buettner, G.R. (2001). Redox environment of the cell as viewed through the redox state of the glutathione disulfide/glutathione couple. *Free Radic. Biol. Med.* 30, 1191–1212.
- Schouten, A., Roosien, J., Bakker, J., and Schots, A. (2002). Formation of disulfide bridges by a single-chain Fv antibody in the reducing ectopic environment of the plant cytosol. *J. Biol. Chem.* 277, 19339–19345.
- Sedlak, T.W., Oltvai, Z.N., Yang, E., Wang, K., Boise, L.H., Thompson, C.B., and Korsmeyer, S.J. (1995). Multiple Bcl-2 family members demonstrate selective dimerizations with Bax. *Proc. Natl. Acad. Sci. USA* 92, 7834–7838.
- Shen, Z.-J., Esnault, S., Schinzel, A., Borner, C., and Malter, J.S. (2009). The peptidyl-prolyl isomerase Pin1 facilitates cytokine-induced survival of eosinophils by suppressing Bax activation. *Nat. Immunol.* 10, 257–265.
- Walensky, L.D., Pitter, K., Morash, J., Oh, K.J., Barbuto, S., Fisher, J., Smith, E., Verdine, G.L., and Korsmeyer, S.J. (2006). A stapled BID BH3 helix directly binds and activates BAX. *Mol. Cell* 24, 199–210.
- Wang, G.-Q., Gastman, B.R., Wieckowski, E., Goldstein, L.A., Rabinovitz, A., Yin, X.-M., and Rabinowich, H. (2001). Apoptosis-resistant mitochondria in T cells selected for resistance to Fas signaling. *J. Biol. Chem.* 276, 3610–3619.
- Wei, M.C., Lindsten, T., Mootha, V.K., Weiler, S., Gross, A., Ashiya, M., Thompson, C.B., and Korsmeyer, S.J. (2000). tBID, a membrane-targeted death ligand, oligomerizes BAK to release cytochrome c. *Genes Dev.* 14, 2060–2071.
- Wei, M.C., Zong, W.X., Cheng, E.H., Lindsten, T., Panoutsakopoulou, V., Ross, A.J., Roth, K.A., MacGregor, G.R., Thompson, C.B., and Korsmeyer, S.J. (2001). Proapoptotic BAX and BAK: a requisite gateway to mitochondrial dysfunction and death. *Science* 292, 727–730.
- Willis, S.N., Chen, L., Dewson, G., Wei, A., Naik, E., Fletcher, J.I., Adams, J.M., and Huang, D.C. (2005). Proapoptotic Bak is sequestered by Mcl-1 and Bcl-xL, but not Bcl-2, until displaced by BH3-only proteins. *Genes Dev.* 19, 1294–1305.
- Willis, S.N., Fletcher, J.I., Kaufmann, T., van Delft, M.F., Chen, L., Czabotar, P.E., Ierino, H., Lee, E.F., Fairlie, W.D., Bouillet, P., et al. (2007). Apoptosis initiated when BH3 ligands engage multiple Bcl-2 homologs, not Bax or Bak. *Science* 315, 856–859.
- Wolter, K.G., Hsu, Y.-T., Smith, C.L., Nechushtan, A., Xi, X.-G., and Youle, R.J. (1997). Movement of Bax from the cytosol to mitochondria during apoptosis. *J. Cell Biol.* 139, 1281–1292.
- Youle, R.J., and Strasser, A. (2008). The BCL-2 protein family: opposing activities that mediate cell death. *Nat. Rev. Mol. Cell Biol.* 9, 47–59.